

## Association of trace elements and dissolution rates of soil iron oxides

D. Ketrot<sup>A,B</sup>, A. Suddhiprakarn<sup>A</sup>, I. Kheoruenromne<sup>A</sup>, and B. Singh<sup>B,C</sup>

<sup>A</sup>Department of Soil Science, Faculty of Agriculture, Kasetsart University, Chatuchak, Bangkok 10900, Thailand.

<sup>B</sup>Faculty of Agriculture and Environment, University of Sydney, NSW 2006, Australia.

<sup>C</sup>Corresponding author. Email: balwant.singh@sydney.edu.au

**Abstract.** In this study, nine Oxisols and five Ultisols from Thailand were used to determine the association of major and trace elements with iron (Fe) oxides. The Fe oxides were concentrated and the association of elements (Al, Ca, Cu, Cr, Mg, Mn, Ni, Pb, P, Si, V, Ti, Zn) with Fe was evaluated using batch dissolution in 1 M HCl at 20°C. The dissolution behaviour of Fe oxide concentrates was determined using batch dissolution and flow-through reactors. In addition to Fe, both Al and Ti were present in significant amounts in the Fe oxide concentrates. Manganese was the most abundant trace element, and Cu, Zn, Pb and As concentrations were <250 mg kg<sup>-1</sup> in most samples. The dissolution behaviour of Fe-oxide concentrates indicated that Al, Cr and V were mostly substituted for Fe<sup>3+</sup> in the structure of goethite and hematite. A significant proportion of Mn, Ni, Co, Pb and Si was also present within the structure of these minerals. Some Mg, Cu, Zn, Ti and Ca was also associated with Fe oxides. The dissolution kinetics of Fe oxide concentrates was well described by three models, i.e. the cube root law, Avrami–Erofejev equation and Kabai equation, with the dissolution rate constants (10<sup>3</sup>*k*) corresponding to the three models ranging from 0.44 to 6.11 h<sup>-1</sup>, from 1.01 to 4.40 h<sup>-1</sup> and from 0.03 to 4.12 h<sup>-1</sup>, respectively. The *k* constants of Fe oxide concentrates in this study were significantly and negatively correlated with the mean crystal dimension derived from [110] and [104] of hematite, the dominant mineral in most samples. The steady-state dissolution rate of a soil Fe-oxide concentrate (sample Kk) was substantially higher than for synthetic goethite under highly acidic conditions; this is possibly due to the greater specific surface area of sample Kk than the synthetic goethite.

**Additional keywords:** acid dissolution, batch method, Fe oxide concentrate, non-stirred flow through reactor method, total element concentration, tropical red soils.

Received 21 March 2013, accepted 2 September 2013, published online 5 February 2014

### Introduction

Iron (Fe) oxides are the most abundant metallic oxides in soils; they are present in various mineral forms depending upon present or past pedogenic conditions (Schwertmann and Taylor 1989). The distribution of Fe oxides in soils is also varied, ranging from a uniform distribution throughout the soil matrix to concentrated forms in segregations such as concretions and mottles (Schwertmann 1991; Singh and Gilkes 1992; Wiriyakitnateekul *et al.* 2007). Because of the variability of the chemical environment in soil during the precipitation of Fe oxides, and their ability to incorporate other trace elements into their structures, Fe oxides are an important source and sink of environmentally significant trace elements. Incorporation of several elements such as cadmium (Cd), cobalt (Co), chromium (Cr), copper (Cu), manganese (Mn), nickel (Ni), titanium (Ti), and zinc (Zn) occurs in the structure of synthetic goethites (Fitzpatrick *et al.* 1978; Lim-Nunez and Gilkes 1987; Singh *et al.* 2002; Cornell and Schwertmann 2003; Huynh *et al.* 2003; Kaur *et al.* 2009a, 2009b), which lends further support to the association of various trace elements with Fe oxides. Trace elements are commonly associated with

Fe oxides in soils; however, it is not known whether these elements occur within a separate phase or substitute for Fe<sup>3+</sup> in the structure of Fe oxides (Singh and Gilkes 1992; Trolard *et al.* 1995). The substitution of aluminium (Al) in soil goethite and hematite has been well established; however, the association of trace elements has received only limited attention (Fontes and Weed 1991; da Motta and Kämpf 1992; Singh and Gilkes 1992; Trakoonyingcharoen *et al.* 2006; Wiriyakitnateekul *et al.* 2007). Singh and Gilkes (1992) suggested that some portions of the Co, Cr, Cu, Mn, Ni and Zn, associated with Fe oxides in soils from south-western Australia, may be present within the structure of the two commonly occurring Fe oxides—goethite and hematite. A close association of trace elements, including Mn, Ni, Cr and vanadium (V), with Fe oxides exists in Thai soils (Wiriyakitnateekul *et al.* 2007). The nature of the association between trace elements and Fe oxides in soils has not been established for several other environmentally important trace elements.

Characterisation of the dissolution behaviour of natural Fe oxides containing several trace elements is important for predicting the availability of trace elements in soil environments.

Dissolution studies of synthetic goethites have shown that factors such as the nature of the substituent metal, the extent of metal substitution, and the structural and morphological properties of minerals have a major control on their dissolution rate (Schwertmann 1991). Individual substitution of Al, Cr and Co into goethite structure decreases the dissolution rate of goethite in HCl (Schwertmann 1984; Lim-Nunez and Gilkes 1987; Ruan and Gilkes 1995). By contrast, the incorporation of Mn into goethite accelerated the dissolution rate compared with pure goethite (Lim-Nunez and Gilkes 1987; Schwertmann 1991; Alvarez *et al.* 2007). More recently, Kaur *et al.* (2010) found that the dissolution rate of single-metal-substituted goethite was in the order: Zn->Pb(II)->Pb(IV)->unsubstituted>Cd->Cr-goethite. They observed complex dissolution behaviour for multi-metal-substituted goethite that was linearly related to steric strains determined from the lattice parameters of the mineral.

The objectives of this study were (i) to evaluate the association of several major and trace elements with Fe oxides in soils from Thailand using HCl dissolution kinetics and total element analysis, and (ii) to study the dissolution rate of soil Fe-oxide concentrates using a batch dissolution method and at the steady-state using flow-through reactors in highly acid solutions.

## Materials and methods

### Fe oxide concentrates and synthetic goethite

Soils from the B horizon of nine Oxisols and five Ultisols from Thailand were used for the study. The soils have developed on basalt, limestone, sandstone or alluvium. Soil descriptions and characteristics, site locations and land use are summarised in Table 1. The clay fraction of the soils was separated by repeated dispersion and sedimentation. Iron-oxide concentrates were

obtained by boiling the clay fractions with 5 M NaOH to remove kaolinite and gibbsite (Singh and Gilkes 1991a).

Random powder X-ray diffraction (XRD) patterns of Fe-oxide concentrates were obtained by scanning from 3 to 80° 2 $\theta$  with a step size of 0.02° at 0.2° min<sup>-1</sup> using Cu K $\alpha$  radiation,  $\lambda = 1.5418 \text{ \AA}$  on a diffractometer (MMA, 35 kV and 28.5 mA; GBC Scientific Equipment Pty Ltd, Hampshire, IL, USA). The proportion of goethite to hematite (Goe/(Goe+Hem)) of Fe-oxide concentrate was estimated by a comparison of peak area of goethite (110) and hematite (104) in XRD patterns. Aluminium substitution was determined from the *c*-axis dimension of the goethite unit cell obtained from d(110) and d(111) and calculated using the relationship: mol% Al = 1730 - 572.0(*c*<sub>0</sub>) (Schulze 1984). For hematite, Al substitution was determined from the *a*-axis dimension of the hematite unit cell obtained from d(110) and calculated using the relationship: mol% Al = 3109 - 617.1*a*<sub>0</sub> (Schwertmann *et al.* 1979). Mean crystallite dimension (MCD) of goethite and hematite were calculated from the width of reflections at half-maximum using the Scherrer formula (Klug and Alexander 1974).

Synthetic goethite used in this study was synthesised by rapidly adding 5 M KOH to 1 M Fe(NO<sub>3</sub>)<sub>3</sub> solution while stirring, and ageing the precipitate for 2 weeks at 40°C (Schwertmann and Cornell 2000). This synthetic goethite was found by XRD to be pure goethite.

### Total element analysis

The Fe-oxide concentrates and synthetic goethite were digested in concentrated HCl at 80°C until all Fe oxides dissolved; anatase and rutile were still present in the residues of the digests. The concentration of Fe, Al, Ca, Cu, Cr, Mg, Mn, Ni, lead (Pb), phosphorus (P), silicon (Si), V, Ti and Zn in the acid digests was determined using an inductively coupled

**Table 1. Soil classification, parent material, horizon, depth, available P and land use of the soil samples used for extracting the Fe-oxide concentrates in this study**

Soil profile/series	Classification <sup>A</sup>	Parent material	Horizon	Depth (cm)	Available P (mg kg <sup>-1</sup> )	Land use
<i>Oxisols</i>						
Chok Chai (Ci)	Rhodic Kandiuustox	Basalt	Bto1	30–51	4.24	Cassava field, jackfruit and mango
Tha Mai1 (Ti1)	Rhodic Kandiuudox	Basalt	Bto2	52–78	22.43	Tropical orchard
Tha Mai2 (Ti2)	Typic Kandiuudox	Basalt	Bto1	67–100	51.41	Tropical orchard
Pak Chong1 (Pc1)	Typic Kandiuustox	Basalt	Bo	20–50	0.18	Mixed deciduous and dipterocarp forest
Pak Chong2 (Pc2)	Rhodic Kandiuustox	Limestone	Bt2	65–90	0.40	Corn left fallow at time of sampling
Ao Luek1 (Ak1)	Typic Kandiuudox	Limestone	Bto3	52–80	0.25	Tropical rainforest, para rubber, coconut and banana
Ao Luek2 (Ak2)	Typic Kandiuudox	Limestone	Bto1	17–42	2.74	Tropical rainforest and tropical orchards
Ao Luek3 (Ak3)	Rhodic Kandiuudox	Limestone	Bto2	40–60	1.00	Tropical rainforest and tropical orchards
Pathiu (Ptu)	Kandiudalfic Eutrudox	Shale/limestone	Bto2	46–75	0.35	Rainforest species under para rubber, local weeds, and fern
<i>Ultisols</i>						
Mae Taeng (Mt)	Typic Kandiuustult	Basic igneous rock	Bt2	80–110	11.96	Teak forest plantation bordered by cassava field
Khao Kho Soil (Kk)	Typic Paleudult	Rhyolitic tuff	Bt1	40–61	0.75	Mixed cropping of para rubber and upland rice
Chum Phuang (Cpg)	Typic Kandiuustult	Red sandstone	Bt3	75–100	1.23	Tree crop plot in experimental field
Yasothon (Yt)	Typic Paleustult	Old local alluvium	Bt3	50–80	0.19	Eucalyptus plantation
Sadao (Sd)	Typic Kandiuudult	Sedimentary rocks	Bt2	57–81	0.30	Coconut

<sup>A</sup>Soil Survey Staff (2006).

plasma-atomic emission spectrometer (ICP-AES, Varian Vista AX CCD; Agilent Technologies, Santa Clara, CA, USA).

#### HCl dissolution kinetics of Fe-oxide concentrate

To determine the nature of the association of trace elements with Fe oxides, dissolution kinetics measurements were obtained by a batch dissolution method in acid solution. Briefly, 250 mg of Fe-oxide concentrate was added with 200 mL of 1 M HCl in a 250-mL plastic bottle, and the samples were shaken on a horizontal shaker (300 rpm) at  $20 \pm 1^\circ\text{C}$ . After 1, 2, 3, 5, 7, 10, 20, 34, 48, 72, 96, 120, 144, 168 and 192 h, 5 mL of the suspension was withdrawn using an automatic pipette. The suspensions were immediately filtered through a 0.22- $\mu\text{m}$  Millipore filter. The filtered solutions were analysed for Fe, Al, Ca, Co, Cu, Cr, Mg, Mn, Ni, Pb, P, Si, V, Ti and Zn using an ICP-AES.

Equations to describe the dissolution kinetics of Fe-oxide concentrates were cube-root law (Hixson and Crowell 1931), Avrami-Erofejev equation (Cornell and Giovanoli 1993) and Kabai equation (Kabai 1973). The cube root law is:

$$\sqrt[3]{W} = \sqrt[3]{W_0} - kt \quad (1)$$

where  $W_0$  and  $W$  are the weight of sample at  $t=0$  and after time  $t$ , respectively, and  $k$  is a rate constant. The Avrami-Erofejev equation is:

$$\sqrt{-\ln(1-\alpha)} = kt \quad (2)$$

where  $\alpha$  is the fraction Fe dissolved at time  $t$ . The Kabai equation is:

$$\ln\left[\ln\frac{C_0}{C_0-C}\right] = a \ln k + a \ln t \quad (3)$$

where  $C_0$  and  $C$  are the amounts of Fe dissolved at  $t=0$  and at time  $t$ , respectively, and  $a$  is a phase-specific constant. A plot of  $\ln[\ln C_0/(C_0 - C)]$  against  $\ln t$  results in a straight line from which  $k$  and  $a$  can be derived.

#### Dissolution rate of soil Fe oxides and synthetic goethite

Non-stirred flow-through reactors were used to evaluate the dissolution rate at the steady-state of a soil Fe oxide (sample Kk) and the synthetic goethite. The specific surface area (SSA) was measured by the BET  $\text{N}_2$  method (Aylmore *et al.* 1970), with values of 129 and 32  $\text{m}^2\text{g}^{-1}$  for sample Kk and synthetic goethite, respectively. The flow-through reactor (46 mL in volume) used in this study has been described previously by Bibi *et al.* (2011). We used 100 mg Fe oxide for the dissolution experiment; the input solution was 0.01 M NaCl, which was prepared by using AR-grade NaCl, and solution pH was adjusted to the required value (1.0, 2.0 and 3.0) by adding AR-grade HCl. The flow rate of the input solution was  $1.6 \pm 0.2 \text{ mL h}^{-1}$ , which was maintained by a Gilson peristaltic pump. The reactors were immersed in a constant-temperature water bath at  $25 \pm 1^\circ\text{C}$ . Output solution was collected after every 12 h, the solution pH was measured immediately using a calibrated pH meter (PHM 210 pH meter; Radiometer Analytical SAS, Villeurbanne, France), and the solution was stored at  $5^\circ\text{C}$  for Fe determination using ICP-AES (detection limit  $0.01 \text{ mg L}^{-1}$ ). The experiment was continued until the steady-state was

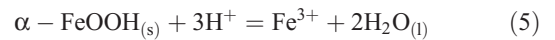
reached, as indicated when the Fe in the output solution remained approximately constant (the difference of at least seven consecutive samples was  $<6\%$ ) (Bibi *et al.* 2011).

The dissolution rate ( $R$ ) of Fe-oxide concentrates and synthetic goethite was calculated following equation below (Cervini-Silva and Sposito 2002; Cheah *et al.* 2003):

$$R = [\text{Fe}] \frac{q}{m} \quad (4)$$

where  $[\text{Fe}]$  is the concentration of Fe in the output solution ( $\mu\text{M}$ ) under steady-state conditions,  $q$  is the solution flow rate ( $\text{L h}^{-1}$ ), and  $m$  is the sample mass in the reactor (kg). The resulting units of  $R$  are then  $\mu\text{mol kg}^{-1} \text{ h}^{-1}$ .

The general reaction (protonation) between protons and goethite can be written as:



The speciation calculations were used to examine the extent of equilibration of the reaction in terms of the Gibbs free energy ( $\Delta G$ ) by using Eqn 6, which was modified from Bibi *et al.* (2011), but the resulting units of  $\Delta G$  are  $\text{kJ mol}^{-1}$ :

$$\Delta G = -5.709 \times \text{SI} \quad (6)$$

where SI is the saturation index of goethite and hematite, calculated using PHREEQC Version 2.18 (Parkhurst and Appelo 1999). The concentration of Fe (see Table 6) in the output solution at the steady-state was used in modelling with PHREEQC to calculate the SI value for the synthetic goethite and Kk samples.

The crystal morphology of both the synthetic goethite and the Kk sample was examined using transmission electron microscopy (TEM) before and after termination of the dissolution at the steady-state. A very dilute suspension of the samples was dispersed by an ultrasonic probe. A drop of suspension was deposited onto a carbon-coated grid and dried at room temperature. Micrographs were obtained using a JEOL 1400 electron microscope (JEOL Ltd, Tokyo).

## Results and discussion

### Mineralogical properties of Fe oxide concentrates

The mineralogical properties of Fe oxide concentrates are shown in Table 2. Hematite and goethite were the main constituents of Fe oxide concentrates from these Thai red soils (Trakoonyingcharoen *et al.* 2006; Wiriyakitnateekul *et al.* 2007). Maghemite, anatase and rutile were present in small amounts in most of the Fe oxide concentrates in the study. The Goe/(Goe + Hem) ratio ranged from 0.12 to 0.74. Most samples had a higher content of hematite than goethite, except for Ti1, Ti2 and Ak1, which had similar amounts of the two minerals. Sample Kk was the only sample where the goethite content exceeded the hematite content. Aluminium substitution in goethite ranged from 10 to 20 mol%, compared with 3–11 mol% Al in hematite in the samples. The substitution of Al in goethite was always greater than the corresponding value for hematite in the same sample. Similar observations were made in earlier studies on highly weathered Brazilian, Australian and Indonesian soils (Fontes and Weed 1991; da Motta and Kämpf

1992; Singh and Gilkes 1992; Prasetyo and Gilkes 1994). The MCD from XRD line-broadening indicated that goethite crystals had a smaller size than associated hematite, as is generally observed for tropical soils (Fontes and Weed 1991; Singh and Gilkes 1992; Prasetyo and Gilkes 1994; Muggler *et al.* 2001; Trakoonyingcharoen *et al.* 2006; Wiriyakitnateekul *et al.* 2007). Aluminium substitution in Fe oxides increases structural strain, slows the rate of crystal growth and reduces crystal size (Schwertmann 1988). Goethite from Ultisols showed similar crystal development along the three crystallographic axes (MCD<sub>110</sub>:MCD<sub>111</sub> close to 1:1). Higher values of MCD along [110] than [104] for hematite indicate better crystal development along X–Y axes compared with the Z-axis; this

is indicative of the platy nature of hematite crystals (Fontes and Weed 1991).

#### Major and trace element concentrations in Fe-oxide concentrates and synthetic goethite

Total element concentrations in the Fe-oxide concentrates and synthetic goethite are presented in Table 3; however, some Ti did not dissolve and persisted as Ti oxides in residues. The concentration of Fe in the concentrates from soils ranged from 389 to 672 g kg<sup>-1</sup>, compared with 632 g kg<sup>-1</sup> in the synthetic goethite. Samples Ci, Kk and Sd had lower Fe concentrations than the other samples, possible due to relatively large amounts

**Table 2. Mineral composition and some properties of goethite and hematite in Fe-oxide concentrates used in this study**  
Hem, Hematite; Goe, goethite; Mhm, maghemite; Ant, anatase; Rut, rutile; MCD, mean crystallite dimension

Sample	Mineral composition	Goe/(Goe + Hem)	Goethite			Hematite		
			Al substitution (%mol)	MCD 110 (nm)	MCD 111 (nm)	Al substitution (%mol)	MCD 104 (nm)	MCD 110 (nm)
<i>Oxisols</i>								
Ci	Hem >> Ant, Goe, Rut, Mhm	0.12	15	–	–	4	16.8	32.1
Ti1	Hem, Goe >> Mhm, Rut	0.47	17	8.1	0.2	9	6.6	8.8
Ti2	Hem, Goe >> Mhm	0.51	17	8.0	0.2	9	6.1	7.0
Pc1	Hem >> Goe, Ant, Mhm, Rut	0.21	20	8.8	0.3	11	11.9	24.3
Pc2	Hem >> Ant, Rut, Goe, Mhm	0.10	14	–	–	9	14.7	28.9
Ak1	Goe, Hem >> Rut, Mhm	0.59	19	14.3	11.7	6	12.3	22.3
Ak2	Hem >> Goe > Rut, Ant, Mhm	0.36	15	12.1	0.2	8	15.5	34.8
Ak3	Hem >> Goe > Ant, Rut, Mhm	0.20	15	7.5	0.2	9	16.0	28.5
Ptu	Hem >> Goe, Ant, Rut, Mhm	0.19	16	11.4	0.2	8	14.2	22.3
<i>Ultisols</i>								
Mt	Hem >> Goe, Rut, Mhm	0.23	13	11.8	11.3	8	15.8	30.1
Kk	Goe >> Hem, Mhm	0.74	16	9.6	8.5	11	7.8	–
Cpg	Hem >> Goe, Ant, Rut, Mhm	0.21	10	14.9	16.2	4	13.5	27.3
Yt	Hem >> Goe > Rut, Mhm, Ant	0.31	10	12.5	13.1	6	12.3	23.4
Sd	Hem >> Goe > Ant ≈ Rut, Mhm	0.36	13	16.5	16.6	3	14.8	23.8

**Table 3. Total element analysis of the soil Fe oxide concentrates and a synthetic goethite used in the study**  
n.d., Not detectable

Sample	Fe	Al (g kg <sup>-1</sup> )	Ti	Mn	Si	Ca	Mg	P	Cu (mg kg <sup>-1</sup> )	Zn	Ni	Cr	V	Pb	As
<i>Oxisols</i>															
Ci	436.9	62.1	42.8	2455	404	223	872	386	34	71	543	381	529	37	n.d.
Ti1	533.3	32.4	82.4	10 500	150	193	1493	1714	116	166	843	184	137	29	8
Ti2	541.2	33.5	89.2	11 278	319	197	1356	1649	128	158	1359	245	161	25	8
Pc1	621.6	22.9	74.3	2396	600	125	529	374	231	111	439	1162	962	28	n.d.
Pc2	671.8	12.0	21.1	3163	516	480	585	453	55	154	723	2038	2312	123	44
Ak1	594.4	43.5	27.0	4171	355	171	860	207	111	244	141	164	1030	112	248
Ak2	560.2	18.3	57.0	5057	450	140	1682	319	83	101	705	339	1367	98	55
Ak3	564.3	33.0	20.6	2891	219	146	1008	335	63	108	368	644	1304	113	243
Ptu	654.0	17.0	21.8	8944	518	228	1222	503	67	149	451	434	1052	120	421
<i>Ultisols</i>															
Mt	633.4	16.5	45.5	3906	514	183	1214	349	75	91	393	694	545	40	n.d.
Kk	501.3	40.2	31.1	10 827	1246	293	6902	338	336	121	132	46	634	41	2
Cpg	559.9	12.3	31.6	4470	322	231	963	606	136	90	173	273	963	174	13
Yt	576.5	12.9	19.9	2669	202	174	1554	350	138	104	310	294	397	111	21
Sd	389.1	15.1	44.7	4070	475	213	1227	218	145	90	295	234	660	101	14
Synthetic goethite	632.1	0.07	0.01	29	652	246	44	n.d.	22	70	26	30	2	n.d.	n.d.

of other minerals (Table 2) and the presence of residual aluminosilicate amorphous phase. Synthetic goethite had negligible to very low concentrations of other elements except Si and Ca, which resulted from the use of glassware in the synthesis. Aluminium and Ti were the major impurities in all Fe-oxide concentrates. Aluminium can be present as a structural substituent for Fe<sup>3+</sup> in goethite and hematite, the two major Fe oxides in the Fe-oxide concentrates (Trakoonyingcharoen *et al.* 2006; Wiriyakitnateekul *et al.* 2007). With the exception of two samples (Ci and Ak3), Fe-oxide concentrates with high content of goethite also contained more Al (Tables 2 and 3), which is consistent with the greater Al substitution in goethite than hematite when they coexist. Aluminium in Ci and Ak3 samples originated from aluminosilicates and was not associated with Fe oxides. Titanium was mostly present in rutile and anatase, which did not fully dissolve in acid; however, some of the Ti can be in Fe oxides (Table 2). Other elements (Mn, Si, Ca, Mg, P, Cu, Zn, Ni, Cr, V, Pb and As) were commonly present in relatively smaller concentrations, with values ranging from below detection to 11 278 mg kg<sup>-1</sup>. Manganese was the most abundant among the other elements, with concentrations of 2396–11 278 mg kg<sup>-1</sup>, whereas the concentrations of Cu, Zn, Pb and As were generally low with values <250 mg kg<sup>-1</sup> in the Fe-oxide concentrates. The high concentrations of Al, Si, Ca and Mg in some of the Fe oxide concentrates (e.g. sample Kk) are possibly due to an amorphous phase, composed mostly of Al and Si, precipitated during the dissolution of clay minerals while obtaining Fe-oxide concentrates; this phase could not be detected by XRD (Singh and Gilkes 1992). Samples Ti1 and Ti2 contained higher amounts of P than the other samples, which is reflected by their relatively high available-P values (Table 1). The Fe-oxide concentrates from soils derived from limestone and shale/limestone had relatively higher concentrations of V and As than the concentrates of soils derived from other parent materials. Darunsontaya *et al.* (2010) also reported high concentrations of V and As in soil clays derived from limestone; As was particularly high in the clay fraction of limestone-derived soils, with values ranging

from 21 to 221 mg kg<sup>-1</sup>, values much larger than for soil clays derived from basalt, sedimentary rock and granite.

Principal component analysis of the total element concentration of Fe-oxide concentrates was used to identify elements and samples that have similar geochemical behaviour. Two factors could explain only ~50% of the variation in the data (Fig. 1a, b). These results are similar to those of Wiriyakitnateekul *et al.* (2007), in which first two factors explained only ~51% of the compositional variations for total element concentrations of Fe-oxide concentrates from Thai soils. They reported that most of the elements measured had a similar chemical behaviour and that Fe oxides in soils derived from basalt had quite different chemical composition from Fe oxides from other soils. However, for this study, the elements could be allocated into four groups, with Zn not belonging to any group (Fig. 1a). The first group included Fe, Cr, V, Pb, As and Ca. These elements had similar geochemical behaviour without systematic differences among soil parent materials. Nevertheless, sample Pc2 differed from other samples due to the high content of Fe-group elements (Fig. 1b). A second group included Si, Mg and Cu, and a third group included Al and Mn caused Kk to differ from other samples. The last group consisted of Ti, P and Ni; these elements were most abundant in samples Ti1 and Ti2, which formed a discrete group, with elevated P being due to fertiliser use.

#### Relationships between trace elements and soil Fe oxides based on HCl dissolution kinetics

Singh and Gilkes (1992) investigated the dissolution kinetics of Fe and trace elements in Fe-oxide concentrates, and based on the shape of the relationship between the proportions of Fe and metal dissolved, they suggested different mechanisms for the associated trace elements with Fe oxides in soils. They proposed that if an element was uniformly distributed throughout Fe-oxide crystals, Fe and the element will dissolve congruently, with a linear relationship and slope equal to 1 in plots of percentage metal v. percentage Fe dissolved, as indicated by line (iv) in

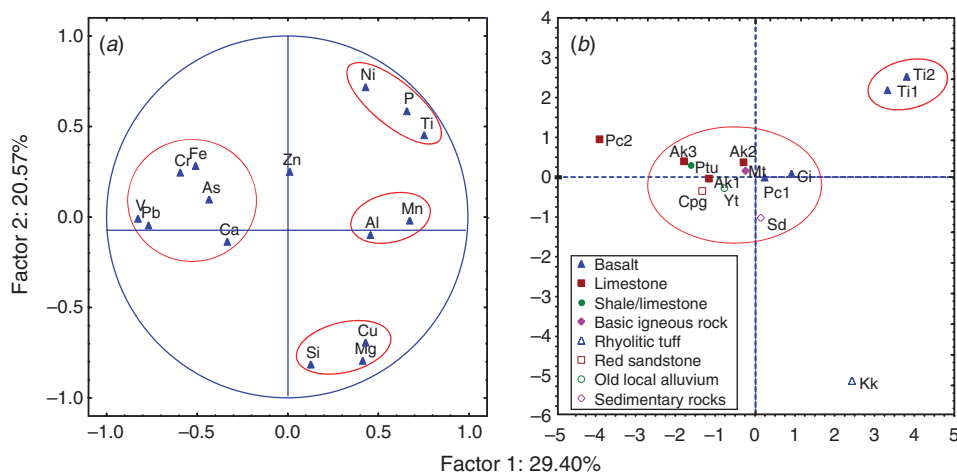


Fig. 1. Factor analysis for total element concentration of the Fe oxide concentrates from Thai red soils derived from different parent materials: (a) elements in Fe oxide concentrates, (b) soil samples.

Fig. 2a. If the element is present as a discrete phase that is very soluble, then 100% of the metal will dissolve before the dissolution of Fe commenced (line (i)). An initial rapid dissolution of a proportion (50%) of the element followed by congruent dissolution with Fe is indicated by line (ii). The converse scenario, where no dissolution of the element commences until 50% of Fe has dissolved, followed by congruent dissolution, is indicated by line (vi). The dissolution behaviour with trend lines similar to lines (ii) and (vi) are likely to indicate that at least 50% of the metal was not associated with Fe oxides. Intermediate behaviours for the association of elements and Fe are shown by the convex curve (iii) and concave curve (v).

The dissolution curves of Al, Cr and V (Fig. 2b, c, d, respectively) showed that for Fe-oxide concentrates, dissolution of these elements and Fe followed a pattern quite similar to the schematic dissolution line (iv) (congruent dissolution) with a few exceptions. For samples Ci and Ak3, Al dissolved faster than Fe (60–80% of Al released), similar to the schematic dissolution lines (i) and (ii), whereas for sample Cpg, Cr dissolved faster than Fe, similar to the schematic dissolution curve (iii). These results suggested that Al (in samples Ci and Ak3) and Cr (in sample Cpg) were present in a discrete phase or were adsorbed onto the surface of Fe-oxide particles, which was consistent with the total Al concentration that was mentioned before. The congruent dissolution of Al, Cr and V with Fe for the majority of samples suggests that these elements are in the structure of goethite and hematite. These metals are known to substitute for Fe<sup>3+</sup> in the structures of goethite and hematite (Trolard *et al.* 1995; Manceau *et al.* 2000; Wells *et al.* 2001; Singh *et al.* 2002; Perrier *et al.* 2006). Aluminium substitution in hematite, the main Fe oxide, in sample Ci (Table 2) was very low but total Al was much higher than in the other samples (Table 3), which suggest that most of the Al in sample Ci was not present in the structure of Fe oxides.

Dissolution behaviour of Mn, Ni, Co, Pb and Si (Fig. 2e, f, g, h, i, respectively) were similar to the schematic dissolution curve (iii) and similar to the results reported for Mn, Ni and Co by Singh and Gilkes (1992). These results indicate that some proportion of Mn, Ni, Co, Pb and Si was present within the structure of Fe oxides. The initial greater release of these elements relative to Fe also suggests that some fraction of the element was present in a discrete solid or soluble phase or adsorbed on to Fe oxides. There are several reports indicating that these elements can be adsorbed by Fe oxides and/or incorporated into Fe-oxide structures (Quin *et al.* 1988; Angove *et al.* 1999; Christophi and Axe 2000; Manceau *et al.* 2000; Wells *et al.* 2006; Kaur *et al.* 2009a; Marcussen *et al.* 2009). The dissolution pattern for Ti was varied (Fig. 2j), showing similarity to schematic dissolution line (ii) and curve (iii). With only a small fraction of the total Ti in Fe-oxide concentrates dissolved during the experiment, we suspect that only a small proportion of Ti was associated with Fe oxides. Most of the Ti that was not dissolved existed in anatase and rutile. The initial faster release of Ti than Fe suggests that a small fraction of Ti was possibly present in nano-crystalline forms of Ti minerals or Ti adsorbed onto Fe oxides.

The dissolution behaviour of Mg, Cu, Zn and Ca (Fig. 2k, l, m, n, respectively) showed an intermediate pattern between lines (i) and (ii) and curve (iii). These results imply that at least 20% of Mg, Zn and Ca and 10% of Cu was not directly associated with Fe oxides. These elements were released during the Fe-oxide concentration process, by oxidation of organic carbon and dissolution of phyllosilicates, and then re-adsorbed onto Fe oxides. Phosphorus did not show any systematic relationship with Fe in the dissolution data (Fig. 2o). However, the greater release of P than Fe during the initial stage of dissolution indicates that some of the P was adsorbed on Fe-oxide surfaces. There are several reports indicating that Fe and Al oxides play a major role in controlling the availability of P in soils through the adsorption–desorption processes (Singh and Gilkes 1991b; Börling *et al.* 2001; Agbenin 2003; Trakoonyingcharoen *et al.* 2005; Wiriyaakitnateekul *et al.* 2005; Wisawapipat *et al.* 2009).

#### *Dissolution rate constant of soil Fe oxides based on HCl dissolution kinetics*

The extent of Fe dissolution plotted against time is shown in Fig. 3. None of the samples was completely dissolved in 1 M HCl at 20°C within the 192-h dissolution period used in the study. The proportion of Fe dissolved at 192 h ranged from 0.07 to 0.42, except for Ti1 and Ti2, with values of 0.59 and 0.62, respectively. The dissolution data for the 14 Fe-oxide concentrates fitted very well to the equations for three models employed (Table 4). The dissolution rate constant ( $10^3k$ ) ranged from 0.44 to 6.11 h<sup>-1</sup> for the cube root law, from 1.01 to 4.40 h<sup>-1</sup> for the Avrami-Erofejev equation and from 0.03 to 4.12 h<sup>-1</sup>, for the Kabai equation. These values are lower than values of  $10^3k$  obtained at 40°C (1 M HCl) for 10 Fe-oxide concentrates from south-western Australia, with values ranging from 10.52 to 35.48 h<sup>-1</sup> for the cube root law and from 7.56 to 32.16 h<sup>-1</sup> for the Kabai equation (Singh and Gilkes 1992). The dissolution rate of goethite and hematite has been known to increase with increasing dissolution temperature, SSA and acid concentration (Chiarizia and Horwitz 1991; Cornell and Giovanoli 1993; Ruan and Gilkes 1995). The values of rate constants are also lower than values (64.8 to 3386.4 h<sup>-1</sup>) reported for the dissolution of six synthetic hematite in 2 M HCl at 65°C obtained using the Avrami-Erofejev equation (Cornell and Giovanoli 1993). Furthermore, values of  $10^3k$  in this study are similar to values for synthetic goethite obtained by the first-order rate equation ( $\ln(1 - \alpha) = -kt$ ) at 25°C with 2 M HCl (7.2 h<sup>-1</sup>), but lower than at 80°C with 1 M HCl (720 h<sup>-1</sup>) and 2 M HCl (4680 h<sup>-1</sup>) (Chiarizia and Horwitz 1991). Similarly, the dissolution rate constants observed in our study are comparable to the values obtained for goethite dissolution ( $3.96 \times 10^3k$  h<sup>-1</sup>) and Al-goethite dissolution ( $3.42$ – $3.96 \times 10^3k$  h<sup>-1</sup>) in 1 M HCl at 30°C for the initial linear part of the graph described by the Kabai equation (Ruan and Gilkes 1995).

The MCD of hematite had significantly negative relationships with dissolution rate constants derived from the three equations. As hematite was the dominant mineral in most of the Fe-oxide concentrates, the crystal size of this mineral has a major influence on the dissolution rate of the Fe-oxide

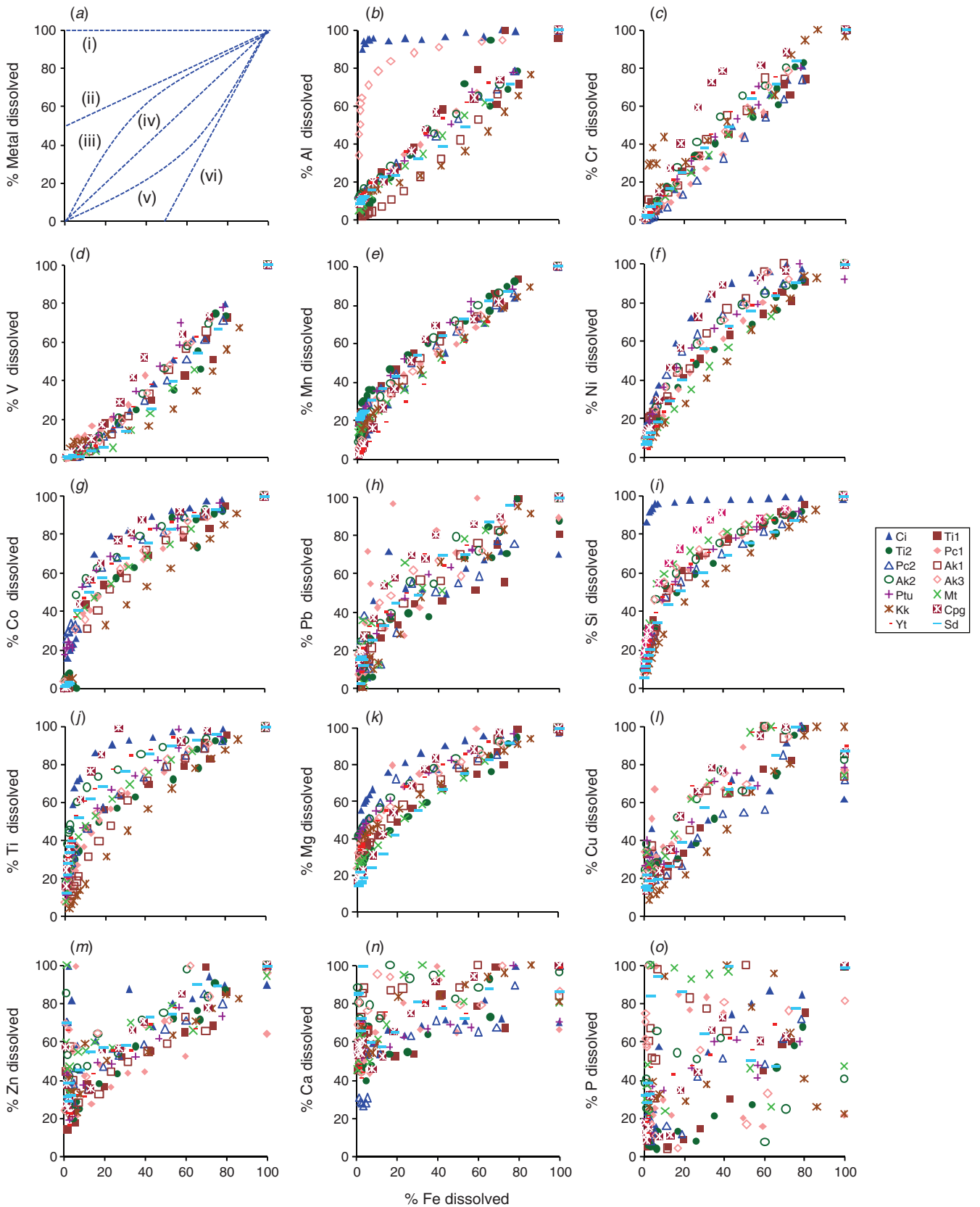


**Fig. 2.** Dissolution of trace elements plotted against Fe dissolved in 1 M HCl at  $20 \pm 1^\circ\text{C}$  at various time intervals for the soil Fe-oxide concentrates: (a) theoretical dissolution behaviours; (b–o) observed dissolution for individual trace elements.

concentrates (Table 5). Several previous studies have shown an inverse relationship between crystal size (and SSA) and the dissolution rate of Fe oxides (Cornell and Giovanoli 1993; Wells *et al.* 2001). Furthermore, Ruan and Gilkes (1995) reported that the dissolution rate of synthetic goethite decreased with increasing Al substitution and increased with increasing dissolution temperature, SSA and heating temperature. Other properties of Fe-oxide concentrates including Goe/(Goe + Hem) ratio, Al substitution in both Fe oxides and MCD of goethite did not show any relationship with the dissolution rate constants (Table 5).

#### Dissolution rate of soil Fe oxides and synthetic goethite at the steady-state

The steady-state dissolution measurement takes several days and requires special equipment, and hence for this measurement, we used only two samples, a synthetic goethite and a goethite-rich soil Fe-oxide concentrate (sample Kk). The dissolution rate

for the two samples was measured using non-stirred flow-through reactors and using 0.01 M NaCl as the electrolyte. The dissolution curve and dissolution rate of synthetic goethite and Kk samples are shown in Fig. 4 and Table 6, respectively. Dissolution of synthetic goethite at pH 1.0 plotted against time (Fig. 4a) showed that the rate of Fe release was rapid during the initial period (up to 83 h) and then decreased before reaching the steady-state (~336 h). Iron release from synthetic goethite was generally low at pH 2.0 and 3.0 (Fig. 4b, c, respectively). The Fe concentration declining with time at pH 1.0 and 2.0 showed no systematic trend at pH 3.0. Little Fe was released rapidly at pH 1.0 from sample Kk (Fig. 4d), but by 80 h a constant rate of dissolution occurred. A similar trend occurred for pH 2.0 (Fig. 4e); however, the steady-state at this pH was reached later (after 288 h) than at pH 1.0. At pH 3.0 (Fig. 4f), Fe release from sample Kk was very low (close to detection limit 0.01 mg L<sup>-1</sup> of ICP-AES) and it increased slowly to reach a steady-state at ~372 h.

The dissolution rate of both the synthetic goethite and Kk samples followed a decreasing trend with solution pH, with the maximum dissolution rate observed at pH 1.0 and the lowest rate at pH 3.0 (Table 6). The dissolution rate of both Fe oxides decreased linearly with increasing solution pH from 1.0 to 3.0 (Fig. 5); however, the effect was more pronounced for sample Kk than the synthetic goethite. The dissolution rate of sample Kk was much greater than the synthetic goethite at pH 1.0 and 2.0, but at pH 3.0 the dissolution rate was similar for the two samples. The much higher dissolution rate of sample Kk than the synthetic goethite at pH 1.0 and 2.0 was possibly due in part to the higher SSA of sample Kk (129 m<sup>2</sup> g<sup>-1</sup>) than the synthetic goethite (32 m<sup>2</sup> g<sup>-1</sup>) (Cornell and Giovanoli 1993; Wells *et al.* 2001). Structural disorder in sample Kk, possibly resulting from the substitution of multiple elements (other than Al), may also have contributed to the higher dissolution rate of this sample compared with the synthetic goethite (Fig. 2). Individual substitutions of foreign elements in the goethite structure are known to produce different effects on

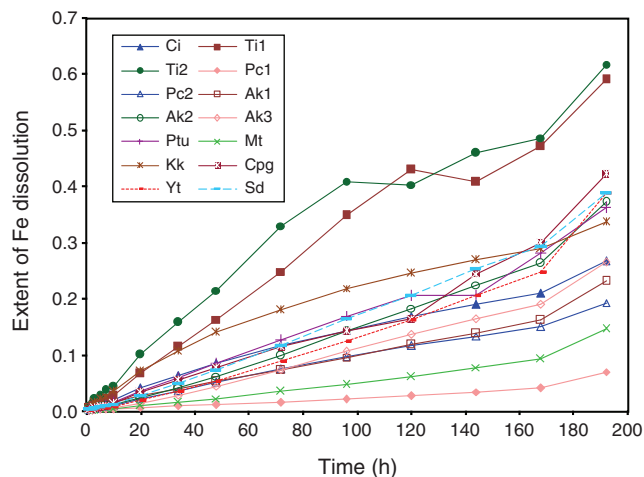


Fig. 3. Cumulative fraction of Fe dissolved in 1 M HCl at 20 ± 1°C from the soil Fe-oxide concentrates during the 192-h batch dissolution experiment.

Table 4. Dissolution parameters of Fe-oxide concentrates derived from the cube-root law, Avrami–Erofejev equation and Kabai equation

\*\*\* $P < 0.001$

Sample	Cube-root law		Avrami–Erofejev eqn		$a$	Kabai eqn	
	$10^3k$ (h <sup>-1</sup> )	$R^2$	$10^3k$ (h <sup>-1</sup> )	$R^2$		$10^3k$ (h <sup>-1</sup> )	$R^2$
Ci	2.19	0.99***	2.39	0.95***	0.77	0.91	0.99***
Ti1	5.87	0.98***	4.40	0.96***	0.97	3.75	0.89***
Ti2	6.11	0.98***	4.33	0.94***	0.88	4.12	0.99***
Pc1	0.44	0.91***	1.01	0.98***	0.65	0.03	0.95***
Pc2	1.55	1.00***	2.07	0.96***	0.85	0.68	0.99***
Ak1	1.70	0.97***	2.06	0.98***	0.70	0.41	0.97***
Ak2	2.99	0.96***	3.05	0.99***	0.94	1.39	0.97***
Ak3	2.10	0.98***	2.60	0.99***	1.05	1.23	0.98***
Ptu	2.99	0.98***	3.00	0.97***	0.94	1.63	0.99***
Mt	1.01	0.94***	1.70	0.99***	0.87	0.35	0.97***
Kk	3.01	0.98***	2.79	0.91***	0.76	1.56	0.99***
Cpg	3.34	0.94***	3.22	0.98***	0.98	1.74	0.98***
Yt	2.94	0.92***	3.06	0.99***	0.99	1.38	0.96***
Sd	3.29	0.98***	3.23	0.99***	0.98	1.74	0.98***

the dissolution of the mineral. For example, the substitution of Mn, Co, Pb and Zn in goethite is known to increase its dissolution rate (Alvarez *et al.* 2005, 2008; Kaur *et al.* 2010), whereas the substitution of Al, Cr and Cd decreased the dissolution rate of goethite (Alvarez *et al.* 2007; Kaur *et al.* 2010). However, the presence of Zn, Pb and Cd in di- and tri-metal (Zn-Pb, Zn-Cd and Zn-Pb-Cd) incorporated goethite

**Table 5. Correlation coefficients for the relationships between some properties of Fe-oxide concentrates and dissolution rate constants ( $10^3k$ )**  
\* $P < 0.05$  and \*\* $P < 0.01$

Property	Cube-root law	Avrami-Erofejev eqn	Kabai eqn
Goe/(Goe + Hem)	0.49	0.42	0.43
Goethite			
Al substitution	-0.07	-0.22	-0.01
MCD 110	-0.22	-0.11	-0.34
MCD 111	-0.21	-0.12	-0.29
Hematite			
Al substitution	-0.07	-0.20	0.04
MCD 104	-0.72*	-0.57	-0.75**
MCD 110	-0.75**	-0.62*	-0.79**

increased the dissolution rate of goethite (Kaur *et al.* 2010). The dissolution rates of the synthetic goethite and Kk samples at pH 3.0 in this study were close to the dissolution rates of goethite at pH 5.0 in the presence of  $200 \mu\text{M}$  oxalate (dissolution rate was  $3.3 \mu\text{mol kg}^{-1} \text{h}^{-1}$ ) reported by Cheah *et al.* (2003).

The approximate steady-state dissolution of the synthetic goethite and Kk samples in this study showed undersaturation with respect to goethite and hematite, with  $\Delta_rG < 0$  (Table 6). The  $\Delta_rG$  for both the synthetic goethite and Kk samples increased with increasing pH. The  $\Delta_rG$  value of synthetic goethite at pH 1.0 and 2.0 was slightly lower than that for Kk, and was very similar at pH 3.0. The  $\Delta_rG$  values of the sample in this study were lower than the  $\Delta_rG$  for goethite dissolution reported by Cheah *et al.* (2003) for various pH values.

As shown by transmission electron micrographs, the crystals of original synthetic goethite were acicular, with particle sizes ranging from around 0.5 to  $2 \mu\text{m}$  (Fig. 6a). For sample Kk, the crystals had a flat, rounded morphology and small size ( $< 20 \text{ nm}$ ) (Fig. 6c), which is consistent with MCD<sub>110</sub> and MCD<sub>111</sub> values of goethite in Table 2. The small crystal size of sample Kk corresponds to higher SSA than for synthetic goethite. There was no observable difference in the crystal size and shape before

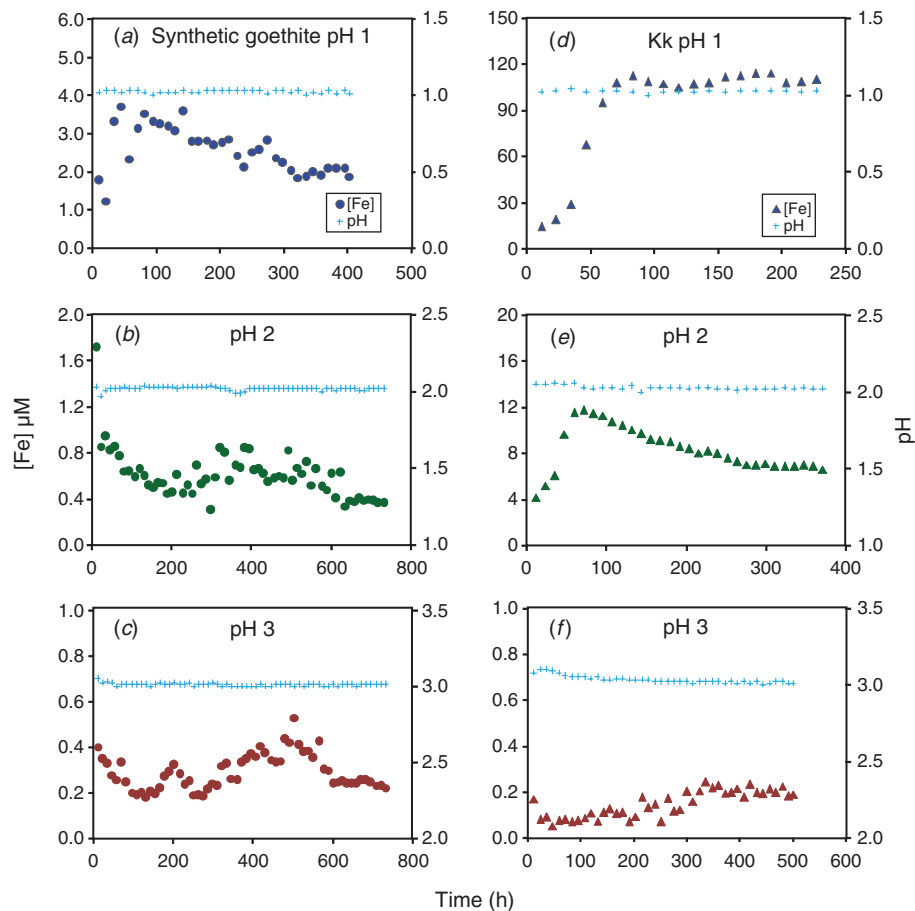


**Fig. 4.** Dissolution behaviour of Fe in  $0.01 \text{ M NaCl}$  at pH 1.0, 2.0 and 3.0 from (a-c) synthetic goethite and (d-f) sample Kk (Fe-oxide concentrate from the Kk soil) using flow-through reactor method at  $25 \pm 1^\circ\text{C}$ .

and after steady-state dissolution was reached at pH 1.0 for either the synthetic goethite (Fig. 6*a, b*) or Kk (Fig. 6*c, d*) samples. Although only a small proportion of the samples was dissolved, nevertheless these observations suggest that there was no selective dissolution along a particular crystal axis of the synthetic and natural samples. Schwertmann (1984) reported that both sides of the lath are attacked by protons, and rounded corrosion features are formed for Al-goethite, but unsubstituted Al-goethite showed preferential dissolution between domains and showed formation of a rhombic holes feature. Furthermore, Cornell and Giovanoli (1993) reported that all crystal faces of hematite dissolved equally well except where susceptible regions were present, and some preferential attack took place

at the (001) faces of the platy crystal, leading to hole formation. Similarly, rounded hematite in soil from south-eastern Ohio (Washington county; 39°28'00"N, 81°33'30"W) exhibited dissolution cavities attributable to instability within the modern pedo-environment (Bigham *et al.* 1991).

**Table 6. Solution pH, flow rate, Fe concentration and dissolution rate (*R*) of synthetic goethite and sample Kk (a soil Fe-oxide concentrate) at the steady-state (with ± s.e.), and  $\Delta_rG$  of reaction**

Sample	pH	Flow rate (mL h <sup>-1</sup> )	[Fe] (μM)	<i>R</i> (μmol kg <sup>-1</sup> h <sup>-1</sup> )	$\Delta_rG$ (kJ mol <sup>-1</sup> )	Goethite	Hematite
Synthetic goethite	1.02	1.63	1.98	32.3 ± 0.5	-62.5	-113.4	
	2.02	1.78	0.39	6.9 ± 0.14	-48.9	-86.4	
	3.01	1.49	0.24	3.6 ± 0.06	-33.1	-54.7	
Kk	1.02	1.41	109.8	1548.4 ± 12.1	-53.1	-94.7	
	2.02	1.40	6.92	96.9 ± 0.5	-42.0	-72.4	
	3.01	1.43	0.20	2.9 ± 0.07	-33.5	-55.6	

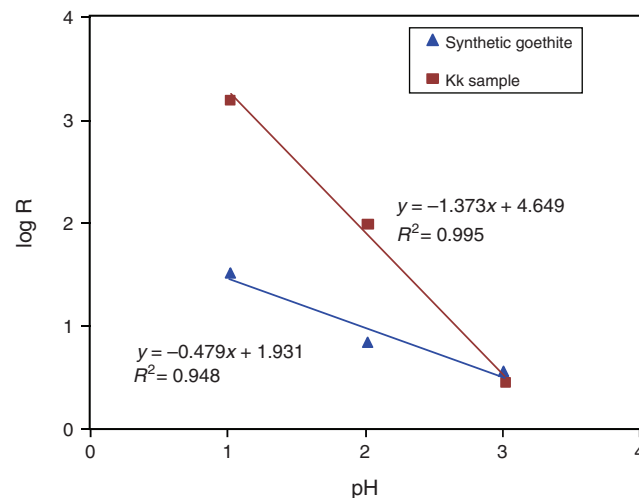


**Fig. 5.** Dissolution rate of a synthetic goethite and an Fe-oxide concentrate from an Ultisol (sample Kk) plotted against solution pH using flow-through reactor method; the experiments were conducted using 0.01 M NaCl background solution at 25 ± 1°C.

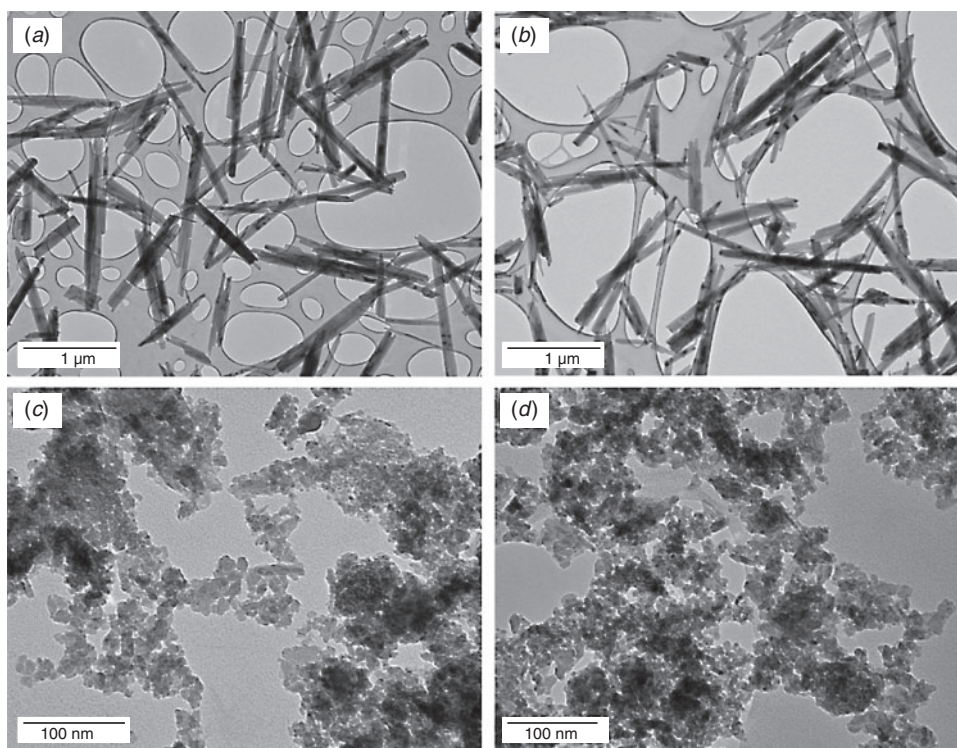


**Fig. 6.** Transmission electron micrographs of (a, b) synthetic goethite and (c, d) an Fe-oxide concentrate from an Ultisol (sample Kk) before and after dissolution (steady-state conditions established), respectively, at pH 1.0 in 0.01 M NaCl.

## Summary and conclusions

Hematite and goethite are abundant Fe oxides in the Oxisols and Ultisols from Thailand examined in this study. Hematite was the dominant Fe oxide in most of the Fe-oxide concentrates of these soils. Iron, Al and Ti were present in significant quantities in the Fe-oxide concentrates. Manganese was the most abundant trace element in the Fe-oxide concentrates. Near-congruency of dissolution indicates that Al, Cr and V are substituted in goethite and hematite structures of most samples. Much of the Mn, Ni, Co, Pb, Si and Ti also appeared to present within the structure of these minerals, whereas Mg, Cu, Zn and Ca were closely associated with Fe oxides but perhaps not substituted in the minerals.

Dissolution behaviour of Fe-oxide concentrates in 1 M HCl at 20°C was well described by the three models investigated. The dissolution rate constant ( $10^3k$ ) values obtained using the three models are lower value than many reported values in the literature, due to the lower concentration of the acid and lower temperature used in our study. The dissolution constants were inversely related to the MCD along [110] and [104] of hematite, the dominant mineral in the Fe-oxide concentrates. The near steady-state dissolution rate of the soil Fe-oxide concentrate (Kk) was much higher than that of the synthetic goethite at pH 1.0 and 2.0; however, at pH 3.0 their dissolution rates were similar. The difference could be partly attributed to the higher SSA of sample Kk than the synthetic goethite. These results may have consequences on the availability of several elements including essential and toxic elements.

The results of this study substantiate the early data obtained for Fe-oxide concentrates for Australian and Thai soils (Singh and Gilkes 1992; Wiriyakitnateekul *et al.* 2007). The results of this study identified that in addition to Al, Cr, Ni, Mn and V, some other elements including Co, Cu and Pb may be associated with Fe oxides in highly weathered soils. Structural incorporation of small (except for Al) and variable amounts of these elements produces structural disorder resulting in much smaller crystal size of goethite and hematite. Our results suggest that Fe oxides isolated from highly weathered soils dissolved at a much faster rate than pure synthetic goethite under highly acidic conditions.

## Acknowledgements

The authors are grateful to The Royal Golden Jubilee PhD Program under The Thailand Research Fund, Kasetsart University and Kasetsart University Research and Development Institute (KURDI) for financial support and to the Faculty of Agriculture and Environment, The University of Sydney, for some laboratory facilities and for staff cooperation and assistance. The authors gratefully acknowledge Dr Nattaporn Prakongkept for the SSA analysis, and Waqar Ahmad and Tom Savage for their help in the total elemental analysis of Fe-oxide concentrates. The authors also acknowledge the facilities as well as scientific and technical assistance from staff in the AMMRF (Australian Microscopy and Microanalysis Research Facility) at the Electron Microscope Unit, The University of Sydney. We thank Bob Gilkes for his critical comments on an earlier version of the manuscript.

## References

Agbenin JO (2003) Extractable iron and aluminum effects on phosphate sorption in a savanna Alfisols. *Soil Science Society of America Journal* **67**, 589–595. doi:10.2136/sssaj2003.0589

- Alvarez M, Sileo EE, Rueda EH (2005) Effect of Mn(II) incorporation on the transformation of ferrihydrite to goethite. *Chemical Geology* **216**, 89–97. doi:10.1016/j.chemgeo.2004.11.004
- Alvarez M, Rueda EH, Sileo EE (2007) Simultaneous incorporation of Mn and Al in the goethite structure. *Geochimica et Cosmochimica Acta* **71**, 1009–1020. doi:10.1016/j.gca.2006.11.012
- Alvarez M, Sileo EE, Rueda EH (2008) Structure and reactivity of synthetic Co-substituted goethites. *The American Mineralogist* **93**, 584–590. doi:10.2138/am.2008.2608
- Angove MJ, Wells JD, Johnson BB (1999) The influence of temperature on the adsorption of cadmium(II) and cobalt(II) on goethite. *Journal of Colloid and Interface Science* **211**, 281–290. doi:10.1006/jcis.1998.6010
- Aylmore LAG, Silis ID, Quirk JP (1970) Surface area of homoionic illite and montmorillonite clay mineral as measured by the sorption of nitrogen and carbon dioxide. *Clays and Clay Minerals* **18**, 91–96. doi:10.1346/CCMN.1970.0180204
- Bibi I, Singh B, Silvester E (2011) Dissolution of illite in saline-acidic solutions at 25°C. *Geochimica et Cosmochimica Acta* **75**, 3237–3249. doi:10.1016/j.gca.2011.03.022
- Bigham JM, Heckendorf SE, Jaynes WF, Smeck NE (1991) Stability of iron oxides in two soils with contrasting colors. *Soil Science Society of America Journal* **55**, 1485–1492. doi:10.2136/sssaj1991.03615995005500050048x
- Börling K, Otabbong E, Barberis E (2001) Phosphorus sorption in relation to soil properties in some cultivated Swedish soils. *Nutrient Cycling in Agroecosystems* **59**, 39–46. doi:10.1023/A:1009888707349
- Cervini-Silva J, Sposito G (2002) Steady-state dissolution kinetics of aluminum-goethite in the presence of desferrioxamine-B and oxalate ligands. *Environmental Science & Technology* **36**, 337–342. doi:10.1021/es010901n
- Cheah SF, Kraemer SM, Cervini-Silva J, Sposito G (2003) Steady-state dissolution kinetics of goethite in the presence of desferrioxamine B and oxalate ligands: implications for the microbial acquisition of iron. *Chemical Geology* **198**, 63–75. doi:10.1016/S0009-2541(02)00421-7
- Chiarizia R, Horwitz EP (1991) New formulations for iron oxides dissolution. *Hydrometallurgy* **27**, 339–360. doi:10.1016/0304-386X(91)90058-T
- Christophi CA, Axe L (2000) Competition of Cd, Cu, and Pb adsorption on goethite. *Journal of Environmental Engineering* **126**, 66–74. doi:10.1061/(ASCE)0733-9372(2000)126:1(66)
- Cornell RM, Giovanoli R (1993) Acid dissolution of hematites of different morphologies. *Clay Minerals* **28**, 223–232. doi:10.1180/claymin.1993.028.2.04
- Cornell RM, Schwertmann U (2003) 'The iron oxides: structure, properties, reactions, occurrences and uses.' 2nd edn (Wiley-VCH Verlag GmbH & Co., KGaA: Weinheim, Germany)
- da Motta PEF, Kämpf N (1992) Iron oxide properties as support to soil morphological features for prediction of moisture regimes in Oxisols of Central Brazil. *Journal of Plant Nutrition and Soil Science* **155**, 385–390. doi:10.1002/jpln.19921550507
- Darunontaya T, Suddhiprakarn A, Kheoruenromne I, Gilkes RJ (2010) Geochemical properties and the nature of kaolin and iron oxides in upland Oxisols and Ultisols under a tropical monsoonal climate, Thailand. *Thai Journal of Agricultural Science* **43**, 197–215.
- Fitzpatrick RW, Roux JL, Schwertmann U (1978) Amorphous and crystalline titanium and iron-titanium oxides in synthetic preparations, at near ambient conditions, and in soil clays. *Clays and Clay Minerals* **26**, 189–201. doi:10.1346/CCMN.1978.0260302
- Fontes MPF, Weed SB (1991) Iron oxides in selected Brazilian Oxisols: I. Mineralogy. *Soil Science Society of America Journal* **55**, 1143–1149. doi:10.2136/sssaj1991.03615995005500040040x
- Hixson AW, Crowell JH (1931) Dependence of reaction velocity upon surface and agitation. I. Theoretical consideration. *Industrial & Engineering Chemistry* **23**, 923–931. doi:10.1021/ie50260a018

- Huynh T, Tong AR, Singh B, Kennedy BJ (2003) Cd substituted goethites—a structural investigation by synchrotron X-ray diffraction. *Clays and Clay Minerals* **51**, 397–402. doi:10.1346/CCMN.2003.0510405
- Kabai J (1973) Determination of specific activation energies of metal oxides and metal oxide hydrates by measurement of the rate of dissolution. *Acta Chimica Academiae Scientiarum Hungaricae* **78**, 57–73.
- Kaur N, Gräfe M, Singh B, Kennedy BJ (2009a) Simultaneous incorporation of Cr, Zn, Cd, and Pb in the goethite structure. *Clays and Clay Minerals* **57**, 234–250. doi:10.1346/CCMN.2009.0570210
- Kaur N, Singh B, Kennedy BJ (2009b) Copper substitution alone and in the presence of chromium, zinc, cadmium and lead in goethite ( $\alpha$ -FeOOH). *Clay Minerals* **44**, 293–310. doi:10.1180/claymin.2009.044.3.293
- Kaur N, Singh B, Kennedy BJ (2010) Dissolution of Cr, Zn, Cd, and Pb single- and multi-metal-substituted goethite: Relationship to structural, morphological, and dehydroxylation properties. *Clays and Clay Minerals* **58**, 415–430. doi:10.1346/CCMN.2010.0580311
- Klug HP, Alexander LE (1974) 'X-ray diffraction procedures for polycrystalline and amorphous materials.' (John Wiley: New York)
- Lim-Nunez R, Gilkes RJ (1987) Acid dissolution of synthetic metal-containing goethites and hematites. In 'Proceedings of the International Clay Conference'. Denver, USA 1985. (Eds LG Schultz, H van Olphen, FA Mumpton) pp. 197–204. (The Clay Mineral Society: Bloomington, IN)
- Manceau A, Schlegel ML, Musso M, Sole VA, Gauthier C, Trolard F (2000) Crystal chemistry of trace elements in natural and synthetic goethite. *Geochimica et Cosmochimica Acta* **64**, 3643–3661. doi:10.1016/S0016-7037(00)00427-0
- Marcussen H, Holm PE, Strobel BW, Hansen HC (2009) Nickel sorption to goethite and montmorillonite in presence of citrate. *Environmental Science & Technology* **43**, 1122–1127. doi:10.1021/es801970z
- Muggler CC, Van Loef JJ, Buurman P, van Doesburg JDJ (2001) Mineralogical and (sub) microscopic aspects of iron oxides in polygenetic Oxisols from Minas Gerais, Brazil. *Geoderma* **100**, 147–171. doi:10.1016/S0016-7061(00)00084-7
- Parkhurst DL, Appelo CAJ (1999) 'User's guide to PHREEQC (version 2)—a computer program for speciation, batch reaction, one-dimensional transport, and inverse geochemical calculations.' Water-Resources Investigations Report No. 99-4259. (U.S. Geological Survey: Reston, VA)
- Perrier N, Gilkes RJ, Colin F (2006) Heating Fe oxide-rich soils increases the dissolution rate of metals. *Clays and Clay Minerals* **54**, 165–175. doi:10.1346/CCMN.2006.0540203
- Prasetyo BH, Gilkes RJ (1994) Properties of iron oxides from red soils derived from volcanic tuff in west Java. *Australian Journal of Soil Research* **32**, 781–794. doi:10.1071/SR9940781
- Quin TG, Long GJ, Benson CG, Mann S, Williams RJP (1988) Influence of silicon and phosphorus on structural and magnetic properties of synthetic goethite and related oxides. *Clays and Clay Minerals* **36**, 165–175. doi:10.1346/CCMN.1988.0360211
- Ruan HD, Gilkes RJ (1995) Acid dissolution of synthetic aluminous goethite before and after transformation to hematite by heating. *Clay Minerals* **30**, 55–65. doi:10.1180/claymin.1995.030.1.06
- Schulze DG (1984) The influence of aluminum on iron oxides. VIII. Unit-cell dimensions of Al-substituted goethites and estimation of Al from them. *Clays and Clay Minerals* **32**, 36–44. doi:10.1346/CCMN.1984.0320105
- Schwertmann U (1984) The influence of aluminium on iron oxides; IX. Dissolution of Al-goethites in 6M HCl. *Clay Minerals* **19**, 9–19. doi:10.1180/claymin.1984.019.1.02
- Schwertmann U (1988) Goethite and hematite formation in the presence of clay minerals and gibbsite at 25°C. *Soil Science Society of America Journal* **52**, 288–291. doi:10.2136/sssaj1988.03615995005200010052x
- Schwertmann U (1991) Solubility and dissolution of iron oxides. *Plant and Soil* **130**, 1–25. doi:10.1007/BF00011851
- Schwertmann U, Cornell RM (2000) 'Iron oxides in the laboratory: preparation and characterization.' 2nd edn (Wiley-VCH Verlag GmbH: Weinheim, Germany)
- Schwertmann U, Taylor RM (1989) Iron oxides. In 'Minerals in soil environments'. (Eds JB Dixon, SB Weed) pp. 379–438, (Soil Science Society of America: Madison, WI)
- Schwertmann U, Fitzpatrick RW, Taylor RM, Lewis DG (1979) The influence of aluminum on iron oxides. Part II. Preparation and properties of Al-substituted hematites. *Clays and Clay Minerals* **27**, 105–112. doi:10.1346/CCMN.1979.0270205
- Singh B, Gilkes RJ (1991a) Concentration of iron oxides from soil clays by 5M NaOH treatment: the complete removal of sodalite and kaolin. *Clay Minerals* **26**, 463–472. doi:10.1180/claymin.1991.026.4.02
- Singh B, Gilkes RJ (1991b) Phosphorus sorption in relation to soil properties for the major soils types of South-Western Australia. *Australian Journal of Soil Research* **29**, 603–618. doi:10.1071/SR9910603
- Singh B, Gilkes RJ (1992) Properties and distribution of iron oxides and their association with minor elements in the soils of south-western Australia. *Journal of Soil Science* **43**, 77–98. doi:10.1111/j.1365-2389.1992.tb00121.x
- Singh B, Sherman DM, Gilkes RJ, Wells MA (2002) Incorporation of Cr, Mn and Ni into goethite ( $\alpha$ -FeOOH): mechanism from extended X-ray absorption fine structure spectroscopy. *Clay Minerals* **37**, 639–649. doi:10.1180/00985502374066
- Soil Survey Staff (2006) 'Keys to Soil Taxonomy.' 10th edn (USDA-Natural Resources Conservation Service: Washington, DC)
- Trakoonyingcharoen P, Kheoruenromne I, Suddhiprakarn A, Gilkes RJ (2005) Phosphate sorption in red Oxisols and red Ultisols in Thailand. *Soil Science* **170**, 716–725. doi:10.1097/01.ss.0000185907.18460.2c
- Trakoonyingcharoen P, Kheoruenromne I, Suddhiprakarn A, Gilkes RJ (2006) Properties of iron oxides in red Oxisols and red Ultisols as affected by rainfall and soil parent material. *Australian Journal of Soil Research* **44**, 63–70. doi:10.1071/SR05025
- Trolard F, Bourrie G, Jeanroy E, Herbillon AJ, Martin H (1995) Trace metals in natural iron oxides from laterites: a study using selective kinetic extraction. *Geochimica et Cosmochimica Acta* **59**, 1285–1297. doi:10.1016/0016-7037(95)00043-Y
- Wells MA, Gilkes RJ, Fitzpatrick RW (2001) Properties and acid dissolution of metal-substituted hematites. *Clays and Clay Minerals* **49**, 60–72. doi:10.1346/CCMN.2001.0490105
- Wells MA, Fitzpatrick RW, Gilkes RJ (2006) Thermal and mineral properties of Al-, Cr-, Mn-, Ni- and Ti-substituted goethite. *Clays and Clay Minerals* **54**, 176–194. doi:10.1346/CCMN.2006.0540204
- Wiriyakitnateekul W, Suddhiprakarn A, Kheoruenromne I, Gilkes RJ (2005) Extractable iron and aluminum predict the P sorption capacity of Thai soils. *Australian Journal of Soil Research* **43**, 757–766. doi:10.1071/SR05026
- Wiriyakitnateekul W, Suddhiprakarn A, Kheoruenromne I, Smirk MN, Gilkes RJ (2007) Iron oxides in tropical soils on various parent materials. *Clay Minerals* **42**, 437–451. doi:10.1180/claymin.2007.042.4.02
- Wisawapipat W, Kheoruenromne I, Suddhiprakarn A, Gilkes RJ (2009) Phosphate sorption and desorption by Thai upland soils. *Geoderma* **153**, 408–415. doi:10.1016/j.geoderma.2009.09.005